Evaluation of spatial resolution of neutron profile monitor in LHD

H. Kawase[1], K. Ogawa[1,2], T. Nishitani[2], N. Pu[1], M. Isobe[1,2], and LHD Experiment Group[2]

[1]SOKENDAI (The Graduate University for Advanced Studies),
322-6 Oroshi-cho, Toki 509-5292, Japan
[2]Natinal Institute for Fusion Science, National Institutes of Natural Sciences,
322-6 Oroshi-cho, Toki 509-5292, Japan

Abstract—**The vertical neutron camera (VNC) has been developed to measure neutron emission profile in deuterium plasmas of the Large Helical Device (LHD). The experiment on spatial resolution evaluation for VNC was carried out in November 2016 by using a ^{252}Cf neutron source of 800 MBq. The neutron source was introduced into the LHD vacuum vessel through an aluminum pipe from an upper diagnostics port to the equatorial plane. The source was placed at the following two positions. The first position is just on the cylindrical collimator axis, and the second position is in the middle of two neighboring collimator axes. The stilbene scintillation detectors are aligned radially at the collimator end to detect unscattered fast-neutrons generated in a deuterium plasma. Three-dimensional neutron transport calculations by using a general-purpose Monte Carlo N-Particle code 6 (MCNP6) reproduced the experimentally obtained neutron counting rate, indicating that VNC has sufficient spatial resolution and the crosstalk between two neighboring collimators is a fairly small fraction. It is expected that the VNC on LHD will function as a tool for study on radial transport of energetic ions.**

***Index Terms*—LHD, deuterium plasma, neutron, neutron camera**

I. Introduction

The Deuterium (D)-Tritium (T) fusion reactions will be used in a future nuclear fusion reactor. Because 3.5 MeV alpha particles born in a D-T plasma play a role as a main heating source in sustaining ignited condition, good confinement of energetic particles is essentially required in magnetic confinement fusion. However, anomalous loss of energetic particle (EP) may occur due to unusual events such as energetic-particle-driven magnetohydrodynamics (MHD) and pressure-driven MHD modes in the future fusion reactor, leading to unwanted localized heat load and/or severe damage on the first wall. Therefore, deep understanding of classical and non-classical behaviors of EPs is important. In currently performed fusion experiments, a plasma is heated by intensive neutral beam injection. In such a circumstance, neutrons are mainly generated by interaction between bulk fuel ions and beam ions. Therefore, neutron emission profile measurement can potentially provide beam ion profile and/or radial transport of beam ion. Because of this, the neutron camera has been employed in large tokamaks producing neutrons, such as the JET [1, 2], the TFTR [3, 4], and the JT-60U [5] in order to measure spatial profile of fusion neutron emission due to beam-plasma interactions. In those devices, EPs transport due to MHD instabilities such as sawteeth and energetic-particle-continuum mode were clearly observed by using the neutron camera [6, 7].

The Large Helical Device (LHD) deuterium plasma was ignited on 7 March 2017. The deuterium operation of LHD offers a new opportunity to extend energetic particle physics study through neutron measurements. In order to investigate radial transport of energetic ions, the vertical neutron camera (VNC) has been developed in LHD [8]. In the design phase of VNC, we used a general-purpose Monte Carlo N-Particle transport code version 6 (MCNP6) [9] to explore a collimator optimized for LHD. The effective spatial resolution of the VNC collimator on LHD was designed so as to be 70 mm [10]. In order to verify performance of VNC in terms of the spatial resolution, the experiment by using an absolutely calibrated spontaneous fission neutron source ^{252}Cf was performed in November 2016. The VNC on LHD is briefly described in Section 2. The experimental scheme is presented in Section 3, together with experimental results. The evaluation of spatial resolution of VNC by using MCNP6 is shown in Section 4. Results from comparison between the experiment and the calculation are shown in Section 5, and the summary of this work is given in Section 6.

II. VNC for the LHD

The overview of VNC on LHD is schematically depicted in Figure 1. The VNC consists of a multichannel collimator made of heavy concrete embedded in the 2.0-Meter thick concrete floor of the LHD torus hall, eleven radially aligned fast-neutron scintillation detectors, and a data acquisition system (DAQ) based on leading edge fast-digitizer equipped

with a field programmable logic circuit (FPGA).

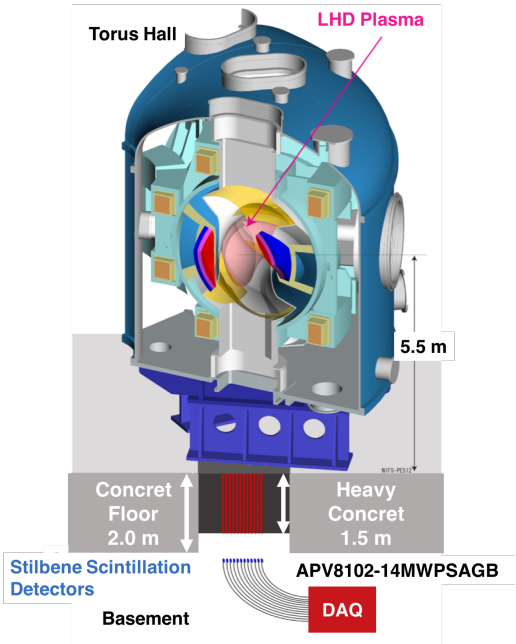

Fig. 1 Schematically drawn overview of vertical neutron camera on LHD. The neutron collimator made of heavy concrete is embedded into the 2.0 m-thick concrete floor of the LHD torus hall. Stilbene detector array is installed at the collimator end in the basement.

The size of the entire multichannel collimator is 0.8 m × 1.4 m and the thickness is 1.5 m. The multichannel collimator consists of heavy concrete and eleven stainless pipes with inner diameter of 30 mm. The heavy concrete of which density is about 3.5 g/cm^3 is made from hematite (Fe_2O_3)-doped concrete. The eleven stainless pipes are embedded in the heavy concrete and radially aligned. Also, the distance of neighboring stainless pipe axes is 90 mm. A stilbene scintillation detector was adopted as a fast-neutron detector in terms of high luminosity, fast response, and good neutron-gamma (n-γ) discrimination capability. The fast-neutron detector for the LHD VNC consists of a stilbene scintillator with ϕ 20 mm and a thickness of 10 mm, and a photomultiplier tube (H11934-100-10MOD: HAMAMATSU Photonics K.K.) with booster power supplies to suppress the gain shift in high-current operation regime [11]. Discrimination between neutron and gamma pulses can be performed from the difference in the pulse shape. As shown in Figure 2, an arbitrary falling time t_1 of the pulse waveform is set appropriately. Subsequently, Q_{long} and Q_{total}(=Q_{short}+Q_{long}) are calculated. Two peaks appear in the histogram of Q_{long}/Q_{total}. One peak with a large value of Q_{long}/Q_{total} results from neutrons, and the other peak corresponds to gamma-rays. The DAQ (Techno-AP Co., Ltd. APV 8102-14 MWPSAGb, V_{pp}: 6 V, 14 bits, DRAM: 2 GB) consists of high-speed sampling (1 GHz) ADC and FPGA, which enable both online and offline n-γ discrimination. The neutron measurement section of VNC on LHD can be stably operated over 10^6 cps to follow rapid events with good statistics on the number of pulse counts.

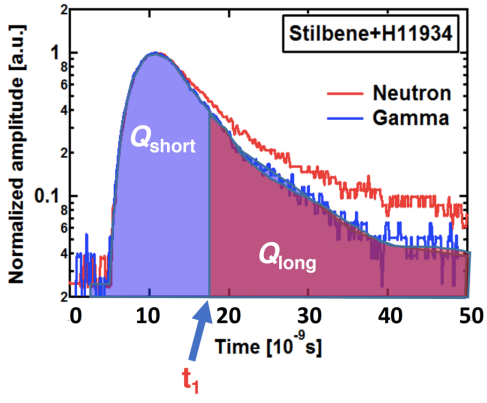

Fig. 2 Pulse shape discrimination method between neutron and gamma-ray pulses. There are two primary decay components. Appropriate t_1 is necessary to obtain good n-γ discrimination.

III. Experimental Setup and Results

A. Experimental setup

The spatial resolution of VNC was evaluated by using an absolutely calibrated neutron source ^{252}Cf with the size of 8 mm in diameter and 10 mm in height in November 2016. The total neutron emission rate of the neutron source in 4π steradian was 8.91×10^7 n/s on the day of the experiment. The neutron source was introduced into the vacuum vessel through an aluminum pipe from an upper diagnostics port. The neutron source is placed at the following two positions by turns. The configuration of this experiment is shown in Figure 3. One position is on the collimator central axis at the major radius R=3.450 m, here designated as the Case-A, and the other position is the middle of two neighboring collimator axes at R=3.405 m, here designated as the Case-B. Also, the vertical position of the source is at the equatorial plane which is 5.5 m from the concrete floor. In this experiment, three stilbene detectors were used at three different positions. Stilbene detectors #1, #2, and #3 were installed at R=3.360 m, 3.450 m, and 4.260 m, respectively.

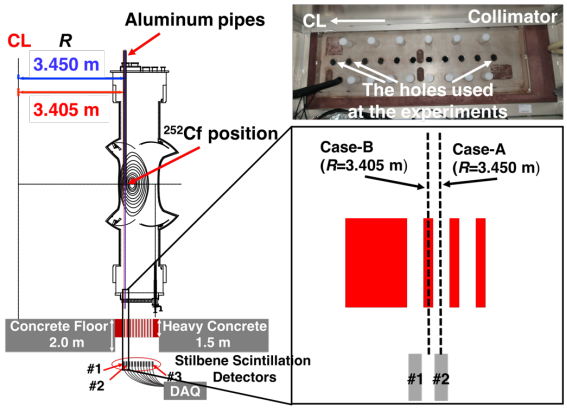

Fig. 3 Configuration of experiment by using ^{252}Cf neutron source and three stilbene scintillation detectors

The purpose of the use of detector #3 was for background measurement. Measurement for many hours was needed to accumulate numbers of pulse counts. In order to avoid data loss due to some accident such as momentary loss of electrical power, we performed one hour measurement repeatedly. In the Case-A, the total measurement time was twelve hours. In the Case-B, the total measurement time was five hours.

B. Experimental results

Pulse shape discrimination between neutron and gamma-ray was performed by using the output waveforms from each detector. Figure 4 shows the n-γ pulse shape discrimination results for the Case-A and the Case-B, respectively. The red curve represents gamma-rays, and the blue curve stands for neutrons corresponding to Q_{long}/Q_{total} from 0.335 to 1. Good n-γ discrimination capability of our detector system can be seen.

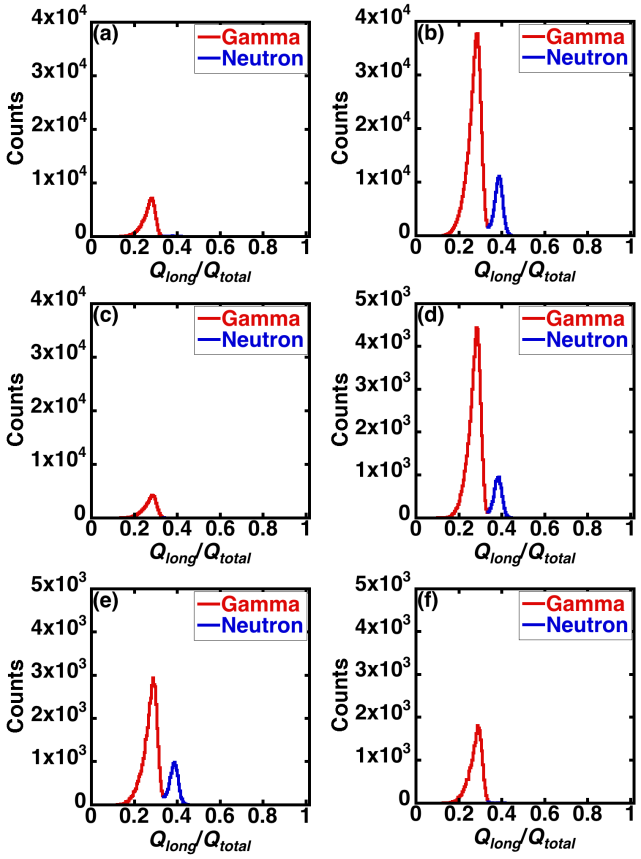

Fig. 4 Results of n-γ discrimination of detectors (a) #1, (b) #2, and (c) #3 in the Case-A and (d) #1, (e) #2, and (f) #3 in the Case-B

In the Case-A, the total neutron counts of #1, #2, and #3 were 891, 104135, and 176, respectively. In the Case-B, the total neutron counts of #1, #2, and #3 were 8853, 9550, and 60, respectively. The neutron pulse counting rates obtained from the experiments are summarized in Table 1.

Table 1 Neutron pulse counting rate obtained in the experiment by using ^{252}Cf source

	Detector #1 [cps]	Detector #2 [cps]	Detector #3 [cps]
Case-A	2.06×10^{-2}	2.41×10^{0}	4.07×10^{-3}
Case-B	4.92×10^{-1}	5.31×10^{-1}	3.33×10^{-3}

In the Case-A, as compared with the neutron pulse counting rate of detectors #1 to that of #2, crosstalk of neutrons coming from adjoined collimator is revealed to be less than 1 %. In the Case-B, the neutron pulse counting rates of detectors #1 and #2 were almost equal as expected because the neutron source was located at the middle of the two neighboring collimators.

IV. Evaluation of Spatial Resolution of VNC by MCNP Calculation

Neutron pulse counting rate of stilbene detector on VNC was predicted by using the MCNP6 code. The calculation model is shown in Figure 5. We performed the neutron transport calculation where a point source with the ^{252}Cf fission spectrum is located on the Case-A and the Case-B. The calculated neutron energy spectra at each detector position are shown in Figure 6. Here, the neutron fluence is normalized by unit source neutron.

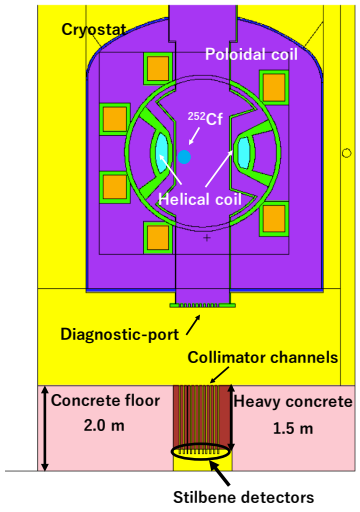

Fig. 5 MCNP calculation model of LHD with VNC.

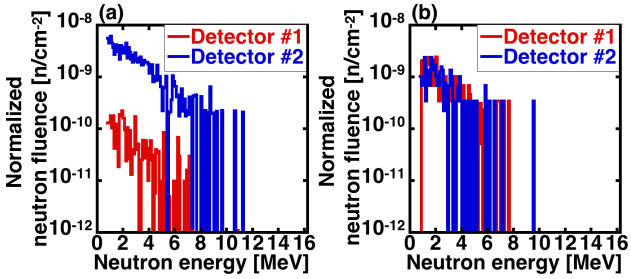

Fig.6 (a) Normalized neutron energy spectra calculated by MCNP6 for the Case-A, (b) Neutron energy spectra for the Case-B.

In the Case-A, the value of normalized neutron fluence integrated in energy of the detectors #1 and #2 are 3.3×10^{-9} n/cm^2 and 1.3×10^{-7} n/cm^2, respectively. In the Case-B, the integrated value of the normalized neutron fluence of detectors #1 and #2 are 3.8×10^{-8} n/cm^2 and 3.4×10^{-8} n/cm^2, respectively. Here we choose the energy range of neutron from 700 keV to 16 MeV. The reason why the lower energy end was chosen to be 700 keV is that because the stilbene scintillation detector is a fast-neutron detector and is not sensitive to neutron below 700 keV according to our test results in the Fast Neutron Laboratory at Tohoku University, Japan. Neutron pulse counting rate of the stilbene detector C cps can be expressed by

$$C \text{ cps} = \text{normalized neutron fluence n/cm}^2 \times \text{neutron emission rate n/s} \times \varepsilon \text{ counts/(n/cm}^2\text{)}$$

Here, the sensitivity of the stilbene scintillation detector to ^{252}Cf source ε is 0.2 counts/n/cm^2, and the neutron emission rate from ^{252}Cf source was 8.91×10^7 n/s on the day of the experiment. The calculation results by using the MCNP6 code are listed in Table 2.

Table 2 Neutron pulse counting rate evaluated by the MCNP6 calculation.

	Detector #1 [cps]	Detector #2 [cps]
Case-A	5.95×10^{-2}	2.26×10^{0}
Case-B	6.77×10^{-1}	6.11×10^{-1}

In the Case-A, as compared with the counting rates of detector #1 to that of detector #2, crosstalk of neutrons coming from adjoined collimator is evaluated to be very small, similar to the experimental results. In the Case-B, the neutron pulse counting rate of detector #1 is almost the same as that of detector #2. This result is also similar to that obtained in the experiment by using the ^{252}Cf neutron source. In Figure 7, comparison between experimental results and calculation results were summarized. The blue dots are experimental results, and the red dots are calculation results.

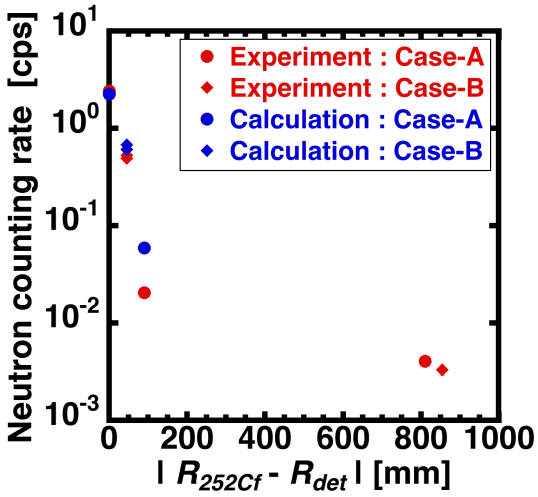

Fig.7 Neutron counting rate profile obtained in experiments and calculation as a function of distance between ^{252}Cf source and detectors.

Here, R_{252Cf} and R_{det} indicate radial positons of ^{252}Cf neutron source and detectors, respectively. This graph indicated that experimental results agree well with calculation results.

V. Summary

Toward the precise measurement of neutron profile in deuterium plasmas of LHD, the spatial resolution of the VNC was evaluated by using a ^{252}Cf neutron source of 800 MBq and MCNP6 code. The neutron source was placed on the collimator axis through aluminum pipes from the upper diagnostics port at vertically elongated poloidal cross section. Subsequently, the neutron source was placed at the middle of two neighboring collimator axes. The measurement by using stilbene detectors placed at the collimator end indicated that the neutron crosstalk between the two neighboring collimators is less than 1 %. The MCNP6 with detailed model of LHD and VNC reproduced the experimentally obtained neutron pulse counting rate. It can be reasonably stated that the VNC on LHD has sufficient spatial resolution for study of fast-ion radial transport.

Acknowledgments

This work was supported by the LHD project budgets (ULHH003, ULHH034, and ULGG801) and JSPS Grant-in-Aid for Scientific Research (B) Grant No. 26289359. This work was partly performed with the support and under the auspices of the NIFS Collaboration Research program (KOAH033).

References

[1] J. M. Adams *et al.*, Nucl. Instrum. Meth. **A329**, 277 (1993).
[2] O. N. Jarvis *et al.*, Fus. Eng. Des. **34-35**, 59, (1997).
[3] A. L. Roquemore *et al.*, Rev. Sci. Instrum. **61**, 3163 (1990).
[4] A. L. Roquemore *et al.*, Rev. Sci. Instrum. **68**, 544 (1997).
[5] M. Ishikawa *et al.*, Rev. Sci. Instrum. **73**, 4237 (2002).
[6] F. B. Marcus *et al.*, Plasma Phys. Control. Fusion **33**, 227 (1991).
[7] M. Ishikawa *et al.*, Nucl. Fusion **45**, 1474 (2005).
[8] K. Ogawa *et al.*, Rev. Sci. Instrum. **85**, 11E110 (2014).
[9] J.T. Goorley *et al.*, Los Alamos National Laboratory, LA-UR-13-22934 (2013).
[10] T. Nishitani *et al.*, Fus Des. Eng. **123**, 1020 (2017).
[11] A. K. Gupta *et al.*, Nucl. Instrum. Meth. **53,** 352 (1967).